On-Wafer High-Frequency Measurement of Mach–Zehnder Modulation Chips Based on Fiber-Free Coupling and Low-Frequency Photodetection

Junfeng Zhu, Xinhai Zou, Chao Jing, Ying Xu, Yali Zhang, Zhiyao Zhang, Yong Liu, *Senior Member, IEEE*, Shangjian Zhang, *Member, IEEE*, and Ninghua Zhu, *Member, IEEE*

***Abstract*— A self-referenced electrical method is proposed for measuring the high-frequency response of electrooptic modulator Mach–Zehnder modulator (MZM) chips based on fiber-free optical coupling and low-frequency photodetection, in which the intrinsic frequency responses including modulation depth and half-wave voltage are both extracted. With the help of two-tone modulation, the wideband combined response of the microwave adapter network and the MZM chip can be extracted by referencing the fixed difference-frequency components in the low-frequency region. Then, microwave fixture removal is implemented for de-embedding the uneven degradation response of the adapter network in terms of the transmission attenuation and the impedance mismatch. Finally, the power leveling technique is used to retrieve the incident microwave power to obtain the intrinsic modulation depth and half-wave voltage of the MZM chip. Frequency response of MZM chip is experimentally obtained up to 70 GHz with fiber-free coupling and sub-MHz photodetection. Our method features fixed low-frequency photodetection for on-wafer characterization of high-speed MZM chips, and it is very promising for automatic and noninvasive probing tests, thanks to the large photosensitive area optical coupling.**

***Index Terms*— Fiber-free coupling, frequency response, low-frequency photodetection, Mach–Zehnder modulator (MZM) chip.**

Manuscript received 9 May 2024; revised 25 June 2024; accepted 1 July 2024. This work was supported in part by the National Natural Science Foundation of China under Grant 61927821, in part by the Science and Technology Program of Chengdu City under Grant 2024-YF06-00010-HZ, and in part by the Basic Research Project of Chongqing Science and Technology Commission under Grant CSTB2022NSCQ-MSX0499. *(Corresponding author: Shangjian Zhang.)*

Junfeng Zhu, Xinhai Zou, Chao Jing, Ying Xu, Yali Zhang, Zhiyao Zhang, Yong Liu, and Shangjian Zhang are with the Research Center for Microwave Photonics, State Key Laboratory of Electronic Thin Films and Integrated Devices, School of Optoelectronic Science and Engineering, University of Electronic Science and Technology of China, Chengdu 610054, China (e-mail: jfzhu@std.uestc.edu.cn; xhzou@uestc.edu.cn; 202311050823@std.uestc.edu.cn; xuying95@std.uestc.edu.cn; ylzhang@uestc.edu.cn; zhangzhiyao@uestc.edu.cn; yongliu@uestc.edu.cn; sjzhang@uestc.edu.cn).

Ninghua Zhu is with the Institute of Intelligent Photonics, Nankai University, Tianjin 300350, China (e-mail: nhzhu@nankai.edu.cn).

Color versions of one or more figures in this article are available at https://doi.org/10.1109/TMTT.2024.3423779.

Digital Object Identifier 10.1109/TMTT.2024.3423779

I. Introduction

MACH–ZEHNDER modulators (MZMs), as key electrical-to-optical converters, are essential in many applications, such as optical communication [1], [2], optical sensing [3], [4], and microwave photonics [5], [6], in which thin-film lithium niobate-based MZM has attracted considerable research attention, thanks to its potential for high performance and compatibility with complementary metal oxide semiconductor (CMOS) fabrication techniques [7], [8]. In particular, heterogeneous integration on silicon enables a full library of functional components for high-level integration; however, it also raises challenges for process monitoring and automatic testing.

In the case of a wafer-level chip under test, the dynamic characteristic should meet the following requirements and preferences: 1) reduce or avoid optical coupling OFF-chip to enable efficient automatic probing, 2) avoid intense and complex module calibrations, and 3) damage-free for the purpose of on-wafer analysis [9], [10]. Optical methods are simple and direct, but the resolution is typically restricted to several GHz by a grating-based optical spectrum analyzer (OSA) [11], [12]. Electrical methods feature high-resolution, such as the electrooptic frequency sweeping (EOFS) method, with the help of an advanced microwave network analyzer (MNA) [13], [14], [15], [16].

The EOFS method obtains the cascaded response of the MZM chip under test and a *golden* (i.e., of known performance) photodetector (PD). Therefore, it requires expensive equipment, such as a light-wave component analyzer (LCA) with built-in *golden* PD [13], [14]. An improved EOFS method is reported, in the case without a *golden* PD, based on the hypothesis that an electro-absorption modulator (EAM) can function as a modulator and PD with the same response [15], [16]. We proposed a self-calibrated electrical method to characterize high-speed optoelectronic devices by a frequency-shifted heterodyne mapping [17]. However, an efficient frequency shifter is still in its infancy to date with silicon photonic integration technology [9]. Recently, we also proposed on-wafer probing kit designs and demonstrated a damage-free, self-calibrated RF characterization of

an integrated silicon photonic transceiver based on heterodyne mixing. Nevertheless, the measuring frequency range of all the above methods is limited by the bandwidth of the assisted PD. Furthermore, the required waveguide-to-fiber coupling causes unstable and time-consuming measurements, due to the high-frequency photodetection.

We demonstrated low-frequency detection methods based on two-tone and bias-swing modulation [18], which achieve self-calibrated frequency response measurement of high-speed MZMs including dual-parallel MZMs via utilizing a low-speed PD. Nevertheless, the major difficulty lies in that the MZMs under test are assumed with a perfect impedance match. It is impractical for measuring ON-chip MZMs and the accuracy will be significantly affected by the multiple reflections resulting from the impedance mismatch of the MZM chips. Therefore, an on-wafer high-frequency measurement that allows tolerant optical coupling and enables low-frequency photodetection, and meanwhile features the robustness to impedance mismatch is still of particular interest.

In this article, we proposed and experimentally demonstrated an on-wafer self-calibrated method for extracting the high-frequency response of the MZM chip utilizing free-space photodetection at low-frequency. In our scheme, two-tone modulated signals applied on the MZM chip beat with each other and generate desired fixed low-frequency components after photodetection, in which the roll-off responsivity calibration of the assisted PD is eliminated. Moreover, the intrinsic parameters including modulation depth and half-wave voltage of the MZM chip can be obtained with robustness to the impedance mismatch based on microwave de-embedding. It is the first time, to the best of our knowledge, that a proof-of-concept high-frequency response measurement of MZM chip with free-space coupling and low-frequency photodetection has been demonstrated. The experiment results are compared to those obtained using conventional methods to verify consistency and accuracy. In contrast to the two-tone and bias-swing modulation method [18], our method not only realizes low-frequency photodetection to measure the high-speed MZM chip but also features robustness to impedance mismatch. Moreover, it is believed to be helpful for on-wafer process monitoring and automatic testing.

II. Operation Principle

As shown in Fig. 1, a continuous light wave from a laser diode (LD) is sent into the MZM chip under test. The two-tone microwave signal $v(t) = V\sin(\omega t + \theta) + V'\sin(\omega' t + \theta')$ is applied on the RF electrode of the MZM chip. Then, the modulated optical signal from the output of the MZM chip can be written as follows:

$$E(t) = E_0 e^{j\omega_c t}\left\{1 + \gamma\exp\left[jm\sin(\omega t + \theta) + jm'\sin\left(\omega' t + \theta'\right) + j\varphi\right]\right\} \quad (1)$$

where E_0 and ω_c are the amplitude and the angular frequency of the optical carrier, respectively, γ and φ are the splitting ratio and the bias phase of the MZM chip, respectively. m and m' represent the modulation depth at the two-tone modulation frequencies ω and ω', respectively, which are determined by

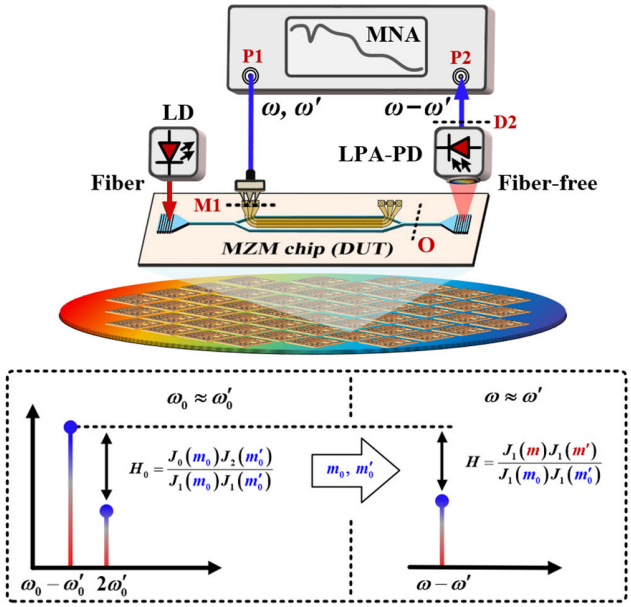

Fig. 1. Schematic of the proposed method, LD, MZM, DUT, LPA-PD, and MNA.

the intrinsic driving power of the MZM chip and can be expressed by the following equation:

$$\begin{aligned} m &= \pi V/V_\pi = \pi|a_{1c}|\sqrt{Z_L}/V_\pi \\ m' &= \pi V'/V'_\pi = \pi\left|a'_{1c}\right|\sqrt{Z_L}/V'_\pi \end{aligned} \quad (2)$$

where V (V'), a_{1c} (a'_{1c}), $V\pi$ ($V'\pi$), and Z_L correspond to the microwave driving amplitude, the incident wave, the half-wave voltage, and the input impedance of the MZM chip, respectively.

To eliminate the roll-off responsivity calibration of the assisted PD and obtain a self-calibrated measurement, the two-tone microwave frequencies are set close to each other. In this case, the half-wave voltages of the MZM chip can be considered to be the same at the two-tone frequencies, i.e., $V_\pi \approx V'_\pi$. Therefore, the following equation can be satisfied:

$$\beta = m/m' = \left|a_{1c}/a'_{1c}\right|. \quad (3)$$

After photodetection, the two-tone modulated optical signal is converted into a photocurrent. With the help of Jacobi–Anger expansion, the photocurrent can be given by the following equation:

$$i(t)/R = E_0^2\left\{\begin{aligned} &1+\gamma^2 \\ &+2\gamma\sum_{k=-\infty}^{+\infty}\sum_{l=-\infty}^{+\infty}J_k(m)J_l\left(m'\right) \\ &\quad\times\cos\left[\left(k\omega + l\omega'\right)t + k\theta + l\theta' + \varphi\right] \end{aligned}\right\} \quad (4)$$

where R is the responsivity of the PD, $J_k(\cdot)$ and $J_l(\cdot)$ are the kth and lth-order Bessel functions of the first kind, respectively. The photocurrent signal contains a series of intermodulation products of the modulation frequencies ω

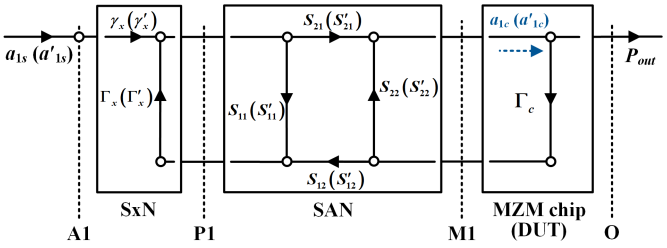

Fig. 2. Signal flow graph among the built-in source network SxN of the MNA, the microwave adapter network: SAN and the MZM chip.

and ω', which can be quantitatively analyzed and mathematically described by the following equation:

$$\begin{aligned} &i\left(k\omega + l\omega'\right) \\ &\quad = 2\gamma E_0^2 R\left(k\omega + l\omega'\right) \\ &\qquad \times \sum_{k=-\infty}^{+\infty} \sum_{l=-\infty}^{+\infty} J_k(m) J_l\left(m'\right) \cos\left(\varphi + \frac{k+l}{2}\pi\right). \end{aligned} \tag{5}$$

From (5), it is easy to quantify the amplitudes of the desired fixed low-frequency signal ($\omega - \omega'$) and a low-frequency reference signal ($2\omega'_0$), given by the following equation:

$$i\left(\omega - \omega'\right) = 4\gamma R\left(\omega - \omega'\right) E_0^2 J_1(m) J_1\left(m'\right) \cos\varphi \tag{6a}$$

$$i\left(2\omega'_0\right) = 4\gamma R\left(2\omega'_0\right) E_0^2 J_0(m_0) J_2\left(m'_0\right) \cos\varphi \tag{6b}$$

where m_0 and m'_0 represent the modulation depth at the two-tone modulation frequencies ω_0 and ω'_0 in the low-frequency region, respectively. The low-frequency reference signal ($2\omega'_0$) is close to the fixed low-frequency $\omega - \omega'$, i.e., $2\omega'_0 \approx \omega - \omega'$, so that $R(2\omega'_0) \approx R(\omega - \omega')$ is satisfied. In this case, a relative amplitude H_0 between the fixed low-frequency signal and the referenced signal can be obtained based on (6a) and (6b) to extract the referenced modulation depths $m_0(\omega_0)$ and $m'_0(\omega'_0)$, given by the following equation:

$$H_0 = \frac{J_0(m_0) J_2\left(m'_0\right)}{J_1(m_0) J_1\left(m'_0\right)}. \tag{7}$$

Therefore, the referenced modulation depth m_0 and m'_0 can be determined based on (3) and (7). Finally, the modulation depths at other modulation frequencies can be extracted from the relative amplitude H of (6a), which is normalized to the referenced modulation depths m_0 and m'_0, given by the following equation:

$$H = \frac{J_1(m) J_1\left(m'\right)}{J_1(m_0) J_1\left(m'_0\right)}. \tag{8}$$

In the same way, the modulation depths can be extracted from (3) and (8) based on the fixed low-frequency components of the two-one modulated optical signal.

To obtain the intrinsic response of the MZM chip, the incident wave a_{1c} (a'_{1c}) should be characterized. Therefore, we investigate and simplify the signal flow graph of the two-tone modulation network as a two-port network, as shown in Fig. 2, where the reference planes A1-M1 include the built-in source network SxN of the MNA and the microwave source adapter network (SAN) connected to the source port. a_{1s} (a'_{1s}) and a_{1c} (a'_{1c}) represent the incident wave at the reference plane A1 and M1, respectively. Γx ($\Gamma' x$) and γ_x (γ'_x) are the reflection coefficient and the transmission coefficient of the source network SxN, respectively, Γ_c is the reflection coefficient of the MZM chip, $[S_{pq}$ (S'_{pq})], $(p, q = 1, 2)$ are the scattering parameters of the microwave adapter network SAN consisting of a microwave combiner (MC) and microwave probe, which delivers electrical signals from the MNA to the MZM chip, O represents the reference plane of the output of the modulated optical carrier.

From Fig. 2, the relationship between a_{1s} (a'_{1s}) and a_{1c} (a'_{1c}) can be determined through the degradation factor $e_{A,M}$ ($e'_{A,M}$) at the reference planes A1-M1, which is denoted as $a_{1c} = a_{1s} \cdot e_{A,M}$ ($a'_{1c} = a'_{1s} \cdot e'_{A,M}$). The degradation factor $e_{A,M}$ ($e'_{A,M}$) can be calculated as follows:

$$\begin{aligned} e_{A,M} &= \frac{a_{1c}}{a_{1s}} \\ &= \frac{\gamma_x \cdot S_{21}}{1 - \Gamma_x S_{11} - S_{22}\Gamma_c - \Gamma_x S_{12} S_{21} \Gamma_c + \Gamma_x S_{11} S_{22} \Gamma_c} \end{aligned} \tag{9a}$$

$$\begin{aligned} e'_{A,M} &= \frac{a'_{1c}}{a'_{1s}} \\ &= \frac{\gamma'_x \cdot S'_{21}}{1 - \Gamma'_x S'_{11} - S'_{22}\Gamma_c - \Gamma'_x S'_{12} S'_{21} \Gamma_c + \Gamma'_x S'_{11} S'_{22} \Gamma_c}. \end{aligned} \tag{9b}$$

In our method, the system correction γ_x (γ'_x) and Γ_x (Γ'_x) are performed at the coaxial port (P1) by using the de-embedding principle that includes the one-port reflection coefficients measurements when the P1 is terminated with three known impedances (Open, Short, Load, i.e., OSL) [19]. Moreover, the scattering parameters of SAN and the reflection coefficient Γ_c of the MZM chip can also be mathematically extracted through the microwave calibration method [20]. In this case, the half-wave voltage of the MZM chip can be extracted based on (2), when the incident wave a_{1S} (a'_{1S}) at the reference plane A1 is determined with the help of the power leveling calibration.

According to theoretical derivation, the measured reference plane is moved from A1 to M1, and the intrinsic modulation depth and half-wave voltage of the MZM chip are determined based on low-frequency photodetection and microwave adapter network de-embedding, which is free of the frequency responses calibration for PD. From (8), the proposed method is also independent of the bias phase φ of the MZM chip. Moreover, the theoretical derivation indicates that our method is applicable for characterizing the MZM including those chips without a good impedance match. When the device under test (DUT) and the adapter network are featured with a good impedance match, the influence of the reflection coefficients Γ_x (Γ'_x), S_{11} (S'_{11}), S_{22} (S'_{22}), and Γ_c can be ignored, and the degradation factor $e_{A,M}$ ($e'_{A,M}$) will degenerate into the transmission attenuation $\gamma_x \cdot S_{21}$ ($\gamma'_x \cdot S'_{21}$) of SxN and SAN. Furthermore, thanks to fixed low-frequency photodetection, the proposed method enables efficient automatic probing by using large photosensitive area free-space coupling instead of waveguide-to-fiber coupling, which is beneficial for automatic on-wafer measurements.

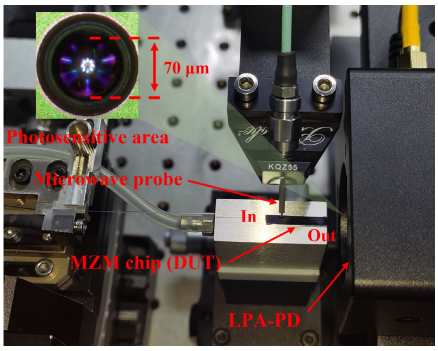

Fig. 3. Experimental setup of the proposed measurement.

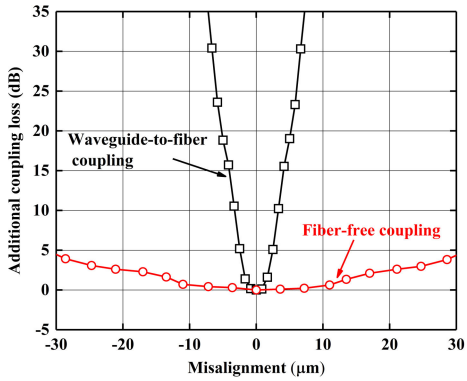

Fig. 4. Additional coupling loss with large photosensitive area PD and SMF pigtailed PD.

III. Experimental Demonstration

In our experiment, we specially choose a thin-film lithium niobate-on-insulator (LNOI) MZM chip to make a comparative measurement in the cases of waveguide-to-fiber coupled photodetection and fiber-free coupled photodetection. Moreover, it is also used for measurement comparisons among the proposed method, the conventional EOFS method, and the OSA method to check the consistency and accuracy.

As shown in Fig. 3, a continuous light wave from an LD is sent into the MZM chip under test and modulated by the 0.3 MHz-spaced (f–f') two-tone signal generated from the MNA source. To realize high alignment tolerance, the optical signal of the MZM chip goes through the output waveguide with a spot size of about 4 μm and is then coupled into a large photosensitive area PD (glgyzn, PD610) with a diameter of about 70 μm. The assisted free-space PD exhibits a responsivity of 0.9 A/W and a 3 dB bandwidth of about 500 MHz. After photodetection, the generated photocurrent is collected by the MNA receiver.

Fig. 4 illustrates the experimentally measured additional coupling loss with large photosensitive area PD (LPA-PD) and single-mode-fiber (SMF) pigtailed PD. When the additional coupling loss is set within 3 dB, the fiber-free coupling allows the misalignment tolerance of ± 25 μm, which is ten times of the waveguide-to-fiber coupling, thanks to the large photosensitive area optical coupling, proving that the fiber-free method can improve the efficiency of the optical coupling.

To obtain the incident wave a_{1c} (a'_{1c}), the system correction of the MNA is first performed at the coaxial port (P1) by using the OSL calibration and power leveling calibration [19],

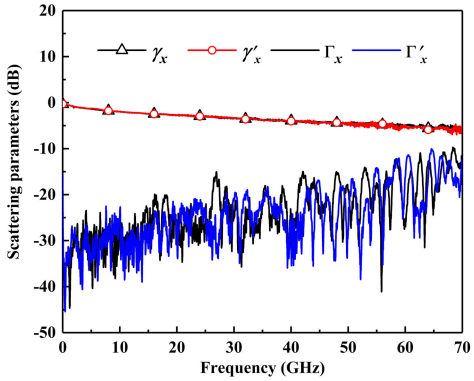

Fig. 5. Measured transmission coefficient γ_x (γ'_x) and reflection coefficient Γ_x (Γ'_x) at the coaxial port P1 of the MNA.

from which the reflection coefficient Γx ($\Gamma' x$), and the transmission coefficient γ_x (γ'_x) of the source network SxN are extracted, as shown in Fig. 5.

After system correction, the reflection coefficients Γ_O (Γ'_O), Γ_S (Γ'_S), Γ_L (Γ'_L) are measured at the coaxial port (P1) when the SAN is terminated with open-short-load impedance substrates (GGB CS-5) at the coplanar tip of the microwave probe, respectively, as shown in Fig. 6(a) and (b). Therefore, the reflection coefficients S_{11} (S'_{11}), S_{22} (S'_{22}), and the transmission coefficients S_{21} (S'_{21}), and S_{12} (S'_{12}) of SAN can be determined based on the microwave calibration method [19], [20], which are shown in Fig. 6(c). It should be noted that since the adapter network SAN is reciprocal, i.e., $S_{21} = S_{12}$ ($S'_{21} = S'_{12}$), the scattering parameters S_{21} and S'_{21} are only presented in Fig. 6(c).

The reflection coefficient Γ_c of the MZM chip can also be extracted from the measured reflection coefficient Γ_M at the coaxial port (P1) when the SAN is terminated with the MZM chip with the assistance of microwave calibration, as shown in Fig. 7. The reflection coefficient Γ_M includes the effect of the scattering parameters of SAN and the reflection coefficient of the MZM chip. It can be found from the Smith chart in Fig. 7 that the SAN introduces a short length of transmission line due to the electronic coupler and on-wafer probe, resulting in the trace rotation and the impedance of the MZM chip located at about 47 Ω. With the scattering parameters of SxN and SAN, the degradation factor $e_{A,M}$ ($e'_{A,M}$) is determined by (9), as shown in Fig. 8. Besides, the incident power a_{1S} (a'_{1S}) of the source network SxN is measured with the power leveling calibration.

Fig. 9(a) shows the referenced electrical spectrum when the two-tone driving frequencies are set as $f_0 = 0.7$ MHz and $f'_0 = 0.4$ MHz, in which the electrical powers are measured to be -16.78 dBm at 0.3 MHz (f_0–f'_0) and -23.17 dBm at 0.8 MHz ($2f'_0$), respectively. With the known incident power a_{1S} (a'_{1S}) and degradation factors $e_{A,M}$ ($e'_{A,M}$) in Fig. 8, the electrical power a_{1c} and a'_{1c} are measured to be 8.71 dBm at 0.7 MHz (f_0) and 8.82 dBm at 0.4 MHz (f'_0), respectively, corresponding to amplitude ratio $\beta = 1.02$ based on (3). With (3) and (7), the referenced modulation depth m_0 and m'_0 are solved to be 0.56 and 0.57 rad, respectively. By the two-tone swept measurement, the combined response of microwave

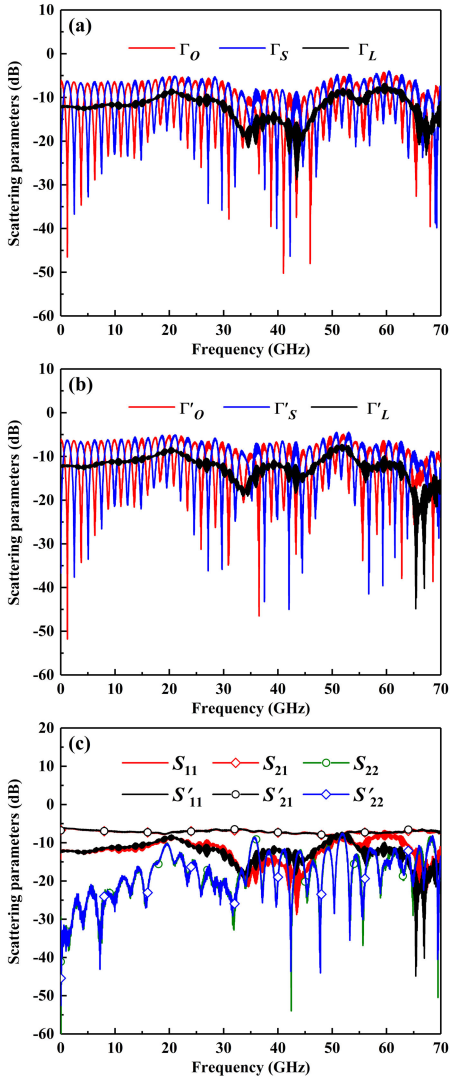

Fig. 6. (a) Measured reflection coefficients Γ_O, Γ_S, Γ_L of the SAN under OSL termination, and modulation frequency f. (b) Measured reflection coefficients Γ'_O, Γ'_S, Γ'_L of the SAN under OSL termination and modulation frequency f'. (c) Extracted scattering parameters of the SAN.

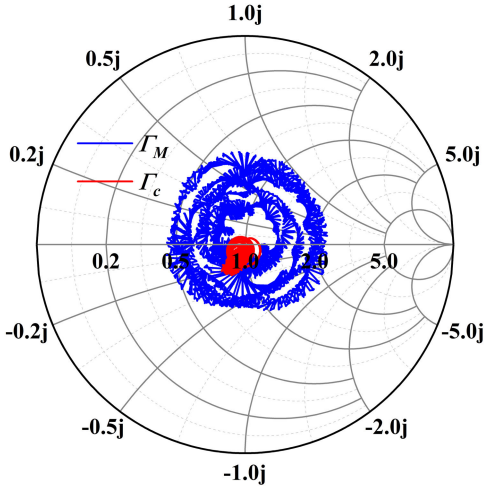

Fig. 7. Measured reflection coefficients on a Smith chart.

adapter network SxN and SAN and the MZM chip can also be measured by detecting the fixed low-frequency signal

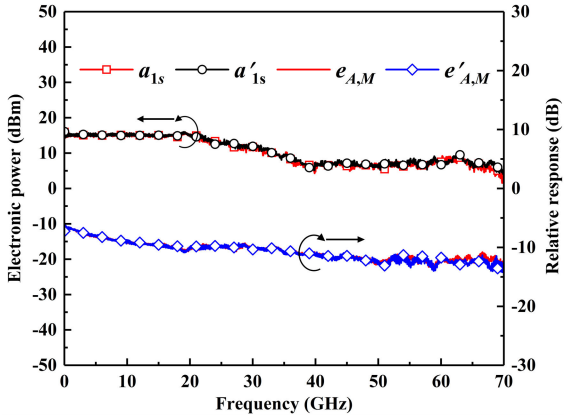

Fig. 8. Measured incident power a_{1S} (a'_{1S}) of source network SxN and degradation factors $e_{A,M}$ ($e'_{A,M}$).

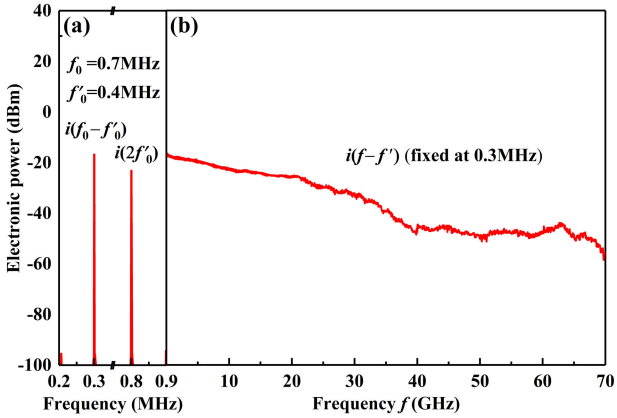

Fig. 9. (a) Measured electrical spectra of the low-frequency reference signal in the case of $f_0 = 0.7$ MHz, $f'_0 = 0.4$ MHz. (b) Measured electrical power of low-frequency signal $f-f'$ (0.3 MHz) under different two-tone modulation frequencies.

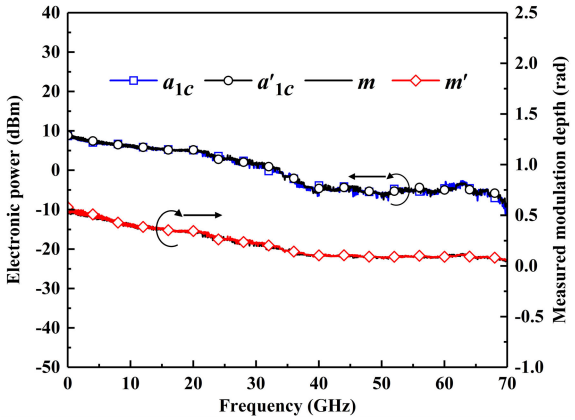

Fig. 10. Measured modulation depths under different frequencies, where microwave driving powers of the two-tone signal are shown for reference.

at $f-f'$, as shown in Fig. 9(b). Thanks to the fixed low-frequency photodetection, the proposed method eliminates the roll-off responsivity of the PD and enables self-calibrated measurement.

Finally, the modulation electrical power a_{1c} (a'_{1c}) and the intrinsic modulation depth m (m') at other modulation frequencies can also be retrieved based on (8) and (9), respectively, as shown in Fig. 10. Meanwhile, the half-wave voltages at

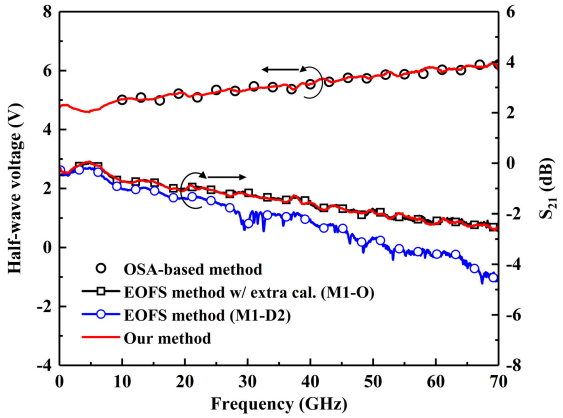

Fig. 11. Measurement results with the OSA method, the EOFS method, and the proposed method.

other modulation frequencies are also obtained based on (2), as illustrated in Fig. 11. To check the accuracy of our method, we make a comparison between the proposed method and the conventional EOFS method. In the conventional EOFS method, the cascaded frequency response of the MZM chip and a broadband PD can be obtained after the generally used microwave calibration procedures of the MNA, as the blue circle line shown in Fig. 11, in which the source and receiver adapter networks are de-embedded, respectively. Then, the individual relative frequency response of the MZM chip can be retrieved from the cascaded frequency response by subtracting the frequency response of PD, as the black square line shown in Fig. 11. It is noteworthy that the frequency response of PD is determined with the help of additional O-E calibration [21]. As shown in Fig. 11, good consistency between the proposed method and the EOFS method with extra O-E calibration is obtained, which confirms that the proposed method achieves the self-referenced frequency response measurement of the MZM chip. For further verification, the half-wave voltage of the MZM chip is also measured with the OSA method. The measured results with the proposed method agree well with that based on the OSA method, as shown in Fig. 11. Note that the OSA method is free of O-E calibration due to the optical domain measurement, but the measurement resolution of the OSA-based method is restricted to be about 2.5 GHz (0.02@1550 nm) by the spectral resolution of the commercially available grating-based OSA. In contrast, our method not only provides the modulation depth, the half-wave voltage, and the relative frequency response with self-calibrated measurement but also features high-resolution measurement.

IV. Discussion and Conclusion

In summary, we have proposed and demonstrated intrinsic frequency response measurement for MZM chips based on fiber-free coupling and low-frequency photodetection. It enables self-referenced measurement of modulation depth, half-wave voltage, and relative frequency response of high-speed MZM chips with robustness to the impedance mismatch. As described in theoretical principles and experimental setups, self-calibration means that our method is independent of any extra calibration of the assistant PD for measuring MZM chips. The modulation depth and half-wave voltage of high-speed MZM chips can be extracted utilizing fixed low-frequency photodetection. Furthermore, the method is promising for automatic and noninvasive measurement, thanks to the large photosensitive area optical coupling.

References

[1] K. Kikuchi, "Fundamentals of coherent optical fiber communications," *J. Lightw. Technol.*, vol. 34, no. 1, pp. 157–179, Jan. 1, 2016.

[2] X. Pang et al., "100 Gbit/s hybrid optical fiber-wireless link in the W-band (75–110 GHz)," *Opt. Exp.*, vol. 9, no. 25, pp. 24944–24949, Nov. 2011.

[3] Y. Yang et al., "Towards fast sensing along ultralong BOTDA: Flatness enhancement by utilizing injection-locked dual-bandwidth probe wave," *Opt. Exp.*, vol. 30, no. 12, pp. 20501–20514, May 2022.

[4] Y. Yan et al., "Dynamic BOTDA based on spectrally efficient frequency-division multiplexing," *J. Lightw. Technol.*, vol. 40, no. 13, pp. 4451–4457, Jul. 2022.

[5] R. Waterhouse and D. Novack, "Realizing 5G: Microwave photonics for 5G mobile wireless systems," *IEEE Microw. Mag.*, vol. 16, no. 8, pp. 84–92, Sep. 2015.

[6] D. Marpaung, J. Yao, and J. Capmany, "Integrated microwave photonics," *Nature Photon.*, vol. 13, no. 2, pp. 80–90, Feb. 2019.

[7] J. Lin, F. Bo, Y. Cheng, and J. Xu, "Advances in on-chip photonic devices based on lithium niobate on insulator," *Photon. Res.*, vol. 8, no. 12, pp. 1910–1936, Dec. 2020.

[8] M. Xu et al., "High-performance coherent optical modulators based on thin-film lithium niobate platform," *Nature Commun.*, vol. 11, no. 1, pp. 3911–3917, Aug. 2020.

[9] S. Zhang, C. Zhang, H. Wang, Y. Liu, J. D. Peters, and J. E. Bowers, "On-wafer probing-kit for RF characterization of silicon photonic integrated transceivers," *Opt. Exp.*, vol. 25, no. 12, pp. 13340–13350, Jun. 2017.

[10] S. Grillanda et al., "Non-invasive monitoring and control in silicon photonics using CMOS integrated electronics," *Optica*, vol. 1, no. 3, pp. 129–136, Aug. 2014.

[11] S. Oikawa, T. Kawanishi, and M. Izutsu, "Measurement of chirp parameters and halfwave voltages of Mach–Zehnder-type optical modulators by using a small signal operation," *IEEE Photon. Technol. Lett.*, vol. 15, no. 5, pp. 682–684, May 2003.

[12] Y. Shi, L. Yan, and A. E. Willner, "High-speed electrooptic modulator characterization using optical spectrum analysis," *J. Lightw. Technol.*, vol. 21, no. 10, pp. 2358–2367, Oct. 2003.

[13] P. D. Hale and D. F. Williams, "Calibrated measurement of optoelectronic frequency response," *IEEE Trans. Microw. Theory Techn.*, vol. 51, no. 4, pp. 1422–1429, Apr. 2003.

[14] P. Debie and L. Martens, "Measuring on-wafer high-frequency modulation response characteristics of optical transmitters and detectors," *IEEE Trans. Instrum. Meas.*, vol. 45, no. 2, pp. 504–510, Apr. 1996.

[15] X. M. Wu et al., "Novel method for frequency response measurement of optoelectronic devices," *IEEE Photon. Technol. Lett.*, vol. 24, no. 7, pp. 575–577, Apr. 2012.

[16] X. Wu, J. Man, L. Xie, J. Liu, Y. Liu, and N. Zhu, "A new method for measuring the frequency response of broadband optoelectronic devices," *IEEE Photon. J.*, vol. 4, no. 5, pp. 1679–1685, Oct. 2012.

[17] S. Zhang et al., "Self-calibrated microwave characterization of high-speed optoelectronic devices by heterodyne spectrum mapping," *J. Lightw. Technol.*, vol. 35, no. 10, pp. 1952–1961, May 15, 2017.

[18] S. J. Zhang, C. Zhang, H. Wang, X. H. Zou, Y. Liu, and J. E. Bowers, "Calibration-free measurement of high-speed Mach–Zehnder modulator based on low-frequency detection," *Opt. Lett.*, vol. 41, no. 3, pp. 460–463, Jan. 2016.

[19] Y. He et al., "High-frequency characterization of electro-optic modulation chips based on photonic down-conversion sampling and microwave fixture de-embedding," *Opt. Exp.*, vol. 30, no. 22, pp. 40337–40346, Oct. 2022.

[20] J. P. Dunsmore, *Handbook of Microwave Component Measurements: With Advanced VNA Techniques*. Hoboken, NJ, USA: Wiley, 2020, pp. 127–181.

[21] M. Wang et al., "Frequency response measurement of high-speed photodiodes based on a photonic sampling of an envelope-modulated microwave subcarrier," *Opt. Exp.*, vol. 29, no. 7, pp. 9836–9845, Mar. 2021.

Junfeng Zhu was born in Chongqing, China, in 1998. He received the B.S. degree from Chongqing University of Posts and Telecommunications, Chongqing, in 2021. He is currently pursuing the Ph.D. degree at the School of Optoelectronic Science and Engineering, University of Electronic Science and Technology of China, Chengdu, China.

His current research interests include microwave photonics and integrated optoelectronic devices.

Xinhai Zou received the Ph.D. degree form the School of Optoelectronic Science and Engineering, University of Electronic Science and Technology of China, Chengdu, China, in 2018.

He is currently an Associate Professor at the School of Optoelectronic Science and Engineering, University of Electronic Science and Technology of China. His research interests include high-speed optoelectronic devices, photonic microwave signal processing, integrated optics, and microwave photonics.

Chao Jing was born in Sichuan, China, in 1996. He received the B.S. and M.S. degrees from the University of Electronic Science and Technology of China, Chengdu, China, in 2019 and 2022, respectively, where he is currently pursuing the Ph.D. degree at the School of Optoelectronic Science and Engineering.

His current research interests include microwave photonics and integrated optoelectronic devices.

Ying Xu was born in Guizhou, China, in 1995. He received the B.S. degree from the University of Electronic Science and Technology of China, Chengdu, China, in 2018, where he is currently pursuing the Ph.D. degree at the School of Optoelectronic Science and Engineering.

His current research interests include microwave photonics and integrated optoelectronic devices.

Yali Zhang received the Ph.D. degree from the Institute of Semiconductors, Chinese Academy of Sciences, Beijing, China, in 2008.

She is currently an Associate Professor with the School of Optoelectronic Science and Engineering, University of Electronic Science and Technology of China, Chengdu, China. Her research interests include optical communications and integrated optics and microwave photonics.

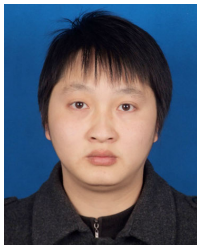

Zhiyao Zhang received the Ph.D. degree from the University of Electronic Science and Technology of China, Chengdu, China, in 2010.

Then, he joined the School of Optoelectronic Science and Engineering, University of Electronic Science and Technology of China. In 2017, he was a Visiting Scholar at the Microwave Photonics Research Laboratory, School of Electrical Engineering and Computer Science, University of Ottawa, ON, Canada. Since 2021, he has been a Full Professor at the University of Electronic Science and Technology of China. His current research interests include microwave photonics and nonlinear fiber optics.

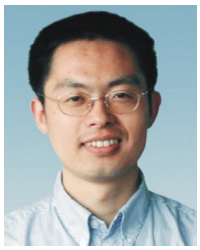

Yong Liu (Senior Member, IEEE) was born in Sichuan, China, in 1970. He received the Ph.D. degree from Eindhoven University of Technology, Eindhoven, The Netherlands, in 2004.

From 1994 to April 2000, he was with the University of Electronic Science and Technology of China, Chengdu, China. In April 2000, he joined the COBRA Research Institute, Eindhoven University of Technology. Since 2007, he has been a Full Professor at the University of Electronic Science and Technology of China. He has co-authored more than 200 journal and conference papers. His research interests include optical nonlinearities and applications, optical signal processing, and optical fiber technologies.

Prof. Liu was a recipient of IEEE Lasers & Electro-Optics Society Graduate Student Fellowship in 2003. He received Chinese National Science Fund for Distinguished Young Scholars in 2009 and Chinese Chang Jiang Scholar in 2013.

Shangjian Zhang (Member, IEEE) received the Ph.D. degree from the Institute of Semiconductors, Chinese Academy of Sciences (CAS), Beijing, China, in 2006.

He was a Visiting Researcher at COBRA, Eindhoven University of Technology, Eindhoven, The Netherlands, and the University of California at Santa Barbara, Santa Barbara, CA, USA. He is a Full Professor at the University of Electronic Science and Technology of China, Chengdu, China. He has authored or co-authored over 140 papers and holds 19 patents. His research interests include high-speed optoelectronic integrated devices and microwave photonic instrumentation.

Ninghua Zhu (Member, IEEE) is currently an Academician with Chinese Academy of Sciences (CAS), Beijing, China, and a Professor at Nankai University, Tianjin, China. He is also the Leader of the National Key Research and Development Program Optoelectronics and Microelectronic Devices, and Integration. In 1998, he was with the Hundred-Talent Program, CAS, and was selected by the National Natural Science Foundation as a Distinguished Young Scientist. He is the Leader in the field of optoelectronics in China. He has authored or co-authored more than 200 journal articles, three books, and three book chapters. He additionally holds 90 patents. His current research interests include the modeling and characterization of integrated optical waveguides and coplanar transmission lines, and optimal design of optoelectronics devices and photonic integrated circuits.

Dr. Zhu was a member of the Ministry of Science and Technology 863 Project. As the first complete person, he was a recipient of the 2013 and 2018 National Award for Technological Invention Second Prize.